

# Water-Oil Displacements from Porous Media Utilizing Transient Adhesion-Tension Alterations

ALAN S. MICHAELS and MARCELLUS C. PORTER

Massachusetts Institute of Technology, Cambridge, Massachusetts

Previous laboratory studies have demonstrated that the injection of small quantities of reverse-wetting agents during water displacement can increase oil recovery from unconsolidated porous media. Hexylamine is a suitable reverse-wetting agent. It has been found that the effectiveness of this treatment increases with the quantity of amine injected (slug volume and/or amine concentration in the slug), and that treatments sufficient to stimulate oil production at high water flow rates did not do so at low flow rates. It has been established that the stimulation of oil production by this technique is accomplished by transient adhesion-tension alterations, resulting in the spontaneous accumulation of oil into large continuous masses which are subsequently mobilized.

The present investigation has attempted to investigate the effect of other variables thought to be important in this system in order to clarify the mechanism by which increased oil recovery is effected. Specifically, the mechanism by which large oil masses are formed and propagated was studied.

Displacement studies conducted in a glass-grid micromodel, under cinemicrographic observation, revealed that large oil masses form as a consequence of restoration of water wettability (amine desorption) but only if the local oil saturation exceeds the irreducible minimum value (under water-wet conditions). Mobilization of these oil masses was observed under the influence of a favorable wettability gradient.

Displacement studies were also performed in unconsolidated silica sand beds, under conditions of varying oil-water viscosity ratio, hydraulic permeability, flow rate, and time at which the amine was injected. In the range of the variables investigated, the additional oil recovered (by treatment) increased as the viscosity ratio increased and as the flow rate or permeability decreased. Early injection of amine also favored increased oil recovery. Water-oil displacement efficiencies enhanced by amine treatment were found to correlate satisfactorily with a parameter representing the ratio of the hydraulic forces to the capillary forces within the medium.

It is generally agreed that the efficiency of a water-oil displacement in a porous medium is limited by capillary forces which trap isolated oil globules. The so-called *irreducible minimum oil saturation* is a measure of oil retained by these forces. Recent estimates (11) indicate that there are about 220 billion barrels of petroleum in United States reservoirs which are not economically recoverable with present techniques such as water flooding. This amounts to almost five times the known recoverable reserves.

It has been recognized for some time that a suitable alteration in the water-oil interfacial tension can result in a better displacement efficiency. Surface-active agents can be used as interfacial tension depressants to accomplish this objective (1, 2, 7, 9), but the additional oil recovery is seldom commensurate with the treatment cost.

It is also recognized that the wettability of the porous medium affects the displacement process (3, 4, 12). Displacements in water-wet systems generally result in lower residual oil saturations than those in oil-wet systems. Wettability alterations resulting in increased oil recovery have received increasing attention in recent years. Leach and Wagner (4, 12) have demonstrated that gross changes in reservoir wettability can be accomplished through chemical treatment of the flood water to change the salinity and pH of the water phase. Increased oil recovery was obtained in both laboratory and field tests with this technique.

Michaels and Timmins (6) studied the effects of transient contact angle alterations resulting from chromatographic transport of reverse-wetting agents through unconsolidated silica sand. It was demonstrated that short chain ( $C_4 - C_8$ ) primary aliphatic amines can improve oil recovery and that the recovery increases with the quantity of amine injected (that is, with either the amine concentration or the volume of the slug injected). Since octyl amine is strongly adsorbed on the sand, it was most effective in altering the wettability but also required the largest throughput of water for desorption. Butyl amine, on the other hand, is only weakly adsorbed and therefore required very little water throughput for desorption but high concentrations for effective wettability reversal.

Michaels and Stancell (8) continued the investigation using hexylamine as the reverse-wetting agent. The additional oil recovery increased monotonically with increasing amounts of amine injected, and it was demonstrated that amine recovery was virtually complete. However, amine slugs of sufficient size and concentration to stimulate oil production at 34 ft./day were found to inhibit production at 4 ft./day. A two-dimensional glass micromodel, simulating a porous medium, was used to study the mechanism by which increased oil recovery was obtained. Microscopic observation in the micromodel and interpretation of data obtained from sand column

experiments indicated that the increase in oil recovery was due to the spontaneous formation of large continuous oil masses, the movement of which was sustained by a favorable wettability gradient across the masses.

The present investigation has attempted to clarify the mechanism by which oil recovery is effected. Specifically, the mechanism by which large oil masses are formed and propagated was studied. In addition to more extensive studies in the micromodel, experiments in unconsolidated sand beds were conducted to investigate three variables:

1. The stage of oil displacement at which amine is injected.
2. The mobility ratio (through variations in oil-phase viscosity).
3. The hydraulic permeability of the porous medium (through variations in sand grain size).

## APPARATUS AND EXPERIMENTAL PROCEDURE

### Macroscopic System

Unconsolidated sand beds were prepared from strongly water-wet silica (Ottawa) sand. The sand was purified prior to use by extensive water wash; treatment with saturated sodium tripolyphosphate solution in order to remove clay; contacting with 1 M hydrochloric acid to remove inorganic

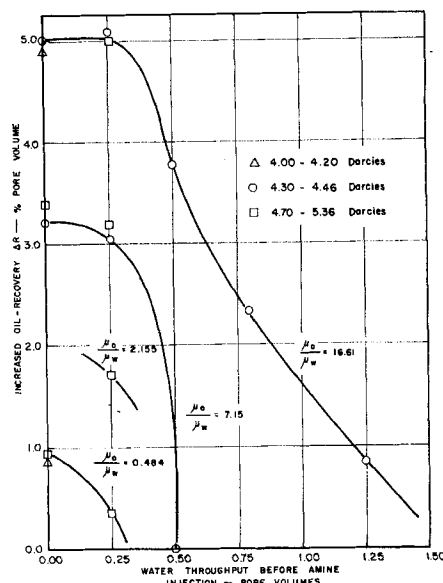


Fig. 1. Effect of injection time and oil-water viscosity ratio on increased oil recovery.

TABLE 1. RUN CONDITIONS

| Run No. | Hydraulic permeability (k), darcies | Viscosity ratio, ( $\mu_o/\mu_w$ ) | Flow rate (v), ft./day | Injection and treatment characteristics†   | Residual oil saturation for untreated flood, % P.V. | $\Delta R$ Change in oil recovery†, % pore volume |
|---------|-------------------------------------|------------------------------------|------------------------|--|---|---|
| 5       | 4.32                                | 7.15                               | 34.0                   | At 0.0 P.V.  | 18.00   | 3.20  |
| 6       | 4.35                                | 7.15                               | 34.0                   | At 0.25 P.V.   | 18.00   | 3.05  |
| 7       | 4.35                                | 7.15                               | 34.0                   | After run 6, inject 0.052 P.V. oil solution of 0.106 N H.A. at 6.7 P.V.                              | 18.00   | 2.05  |
| 8       | 4.70                                | 7.15                               | 34.0                   | At 0.25 P.V.   | 18.00   | 3.18  |
| 9       | 5.17                                | 7.15                               | 34.0                   | At 0.00 P.V.   | 18.00   | 3.38  |
| 10      | 4.30                                | 7.15                               | 34.0                   | At 0.50 P.V.   | 18.00   | 0.00  |
| 11      | 4.32                                | 7.15                               | 34.0                   | At 0.25 P.C. nonuniform porosity   | 18.00   | 3.40  |
| 12      | 5.18                                | 0.485                              | 34.0                   | At 0.0 P.V.  | 18.09   | 0.93  |
| 13      | 5.18                                | 0.485                              | 34.0                   | After run 12, inject H.A. again at 2.92 P.V. Then 0.052 P.V. of 0.1 N hydrochloric acid at 3.96 P.V. | 18.09   | 1.25  |
| 14      | 4.86                                | 2.155                              | 34.0                   | At 0.25 P.V.   | 17.95   | 1.70  |
| 15      | 4.44                                | 16.61                              | 34.0                   | At 0.50 P.V.   | 17.88   | 3.78  |
| 16      | 4.30                                | 16.61                              | 34.0                   | At 0.0 P.V.  | 17.88   | 5.00  |
| 17      | 4.70                                | 16.61                              | 34.0                   | At 0.25 P.V.   | 17.88   | 5.00  |
| 18      | 4.00                                | 16.61                              | 34.0                   | At 0.0 P.V.  | 17.88   | 4.91  |
| 19      | 4.46                                | 16.61                              | 34.0                   | At 0.25 P.V.   | 17.88   | 5.08  |
| 20      | 4.40                                | 16.61                              | 34.0                   | At 0.80 P.V.   | 17.88   | 2.33  |
| 21      | 4.33                                | 16.61                              | 34.0                   | At 1.25 P.V.   | 17.88   | 0.84  |
| 22      | 4.20                                | 0.485                              | 34.0                   | At 0.00 P.V.   | 17.95   | 0.85  |
| 26      | 5.36                                | 0.485                              | 34.0                   | At 0.25 P.V.   | 17.95   | 0.35  |
| 28      | 4.62                                | 0.485                              | 34.0                   | At 0.0 P.V. oil solution of H.A.   | 17.95   | 0.35  |
| 29      | 4.50                                | 0.485                              | 34.0                   | At 0.0 P.V. oil solution of H.A. followed by 0.052 P.V. of 0.1 N hydrochloric acid                   | 17.95   | 2.08  |
| 32      | 2.36                                | 7.15                               | 18.60                  | At 0.00 P.V.   | 17.25   | 3.75  |
| 33      | 1.94                                | 7.15                               | 15.25                  | At 0.00 P.V.   | 17.18   | 3.95  |
| 34      | 23.90                               | 7.15                               | 34.0                   | At 0.00 P.V.   | 17.90   | 4.70  |
| 35      | 14.10                               | 7.15                               | 110.8                  | At 0.00 P.V.   | 20.45   | 2.33  |
| 36      | 15.50                               | 7.15                               | 47.7                   | At 0.00 P.V.   | 18.60   | 3.75  |
| 37      | 15.60                               | 7.15                               | 64.5                   | At 0.00 P.V.   | 19.25   | 3.25  |
| 38      | 15.24                               | 0.485                              | 64.5                   | At 0.00 P.V.   | 19.26   | 0.83  |
| 39      | 15.40                               | 0.485                              | 34.0                   | At 0.00 P.V.   | 17.93   | 1.14  |
| 40      | 15.52                               | 0.485                              | 116.2                  | At 0.00 P.V.   | 20.48   | 0.58  |
| 41      | 14.75                               | 16.60                              | 64.5                   | At 0.00 P.V.   | 19.30   | 4.85  |
| 42      | 16.00                               | 16.60                              | 34.0                   | At 0.00 P.V.   | 18.10   | 6.49  |

\* All treatments = 0.052 P.V. of 0.106 N hexyl amine (H.A.).

† Error estimated as  $\pm 0.1\%$ .

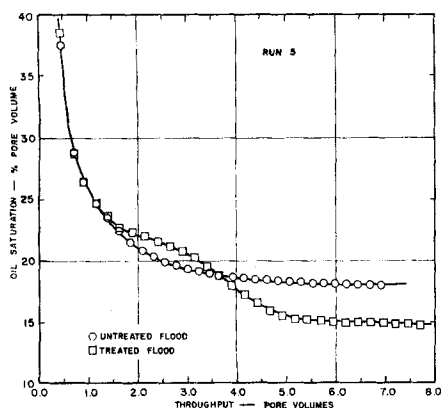


Fig. 2. Oil desaturation curve (medium oil-water viscosity ratio).

oxides, sulfides, and carbonates; treatment with 3% hydrogen peroxide followed by prolonged water washing in order to oxidize and remove organic impurities; and drying in an oven at 150°C. Four sands of different grain size but similar shape were used in this study:

1. 200 to 325 mesh Average grain diameter =  $88 \mu$   
packed porosity =  $35.3 \pm 0.1\%$
2. 140 to 200 mesh Average grain diameter =  $134 \mu$   
packed porosity =  $35.2 \pm 0.2\%$
3. 80 to 100 mesh Average grain diameter =  $221 \mu$   
packed porosity =  $35.9 \pm 0.1\%$
4. 60 to 80 mesh Average grain diameter =  $258 \mu$   
packed porosity =  $36.4\%$

The sand was packed under water in a 2-in. I.D., 2 ft. long glass column mounted on a vibrator. The column was equipped with a tapered end section to minimize the capillary end effect. The pressure drop across the end section was approximately 60% of the total pressure drop across the bed and contained approximately 0.02% of the total bed volume. The porosity was determined from the volume of water added and from the sand density and total weight. The hydraulic permeability was determined by measuring the pressure drop across the column at a given flow rate of water. The uniformity of the pack was checked for oils more viscous than water by recording the variation in pressure drop with time during oil saturation. If the variation was discontinuous rather than linear, the column was discarded (with the exception of that used in run 11).

Oil was prepared by blending purified white (light) paraffin oil and *n*-heptane in the proper ratio to give the desired vis-

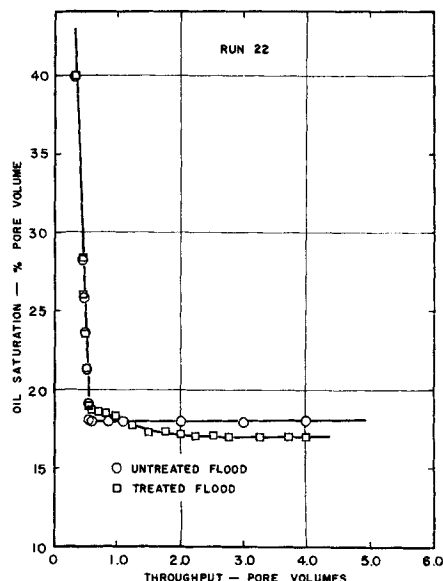


Fig. 4. Oil desaturation curve (low oil-water viscosity ratio).

cosity. The viscosity was measured in a viscometer at 35°C. Four different viscosities were used in this study: 0.35, 1.557, 5.16, and 12.16 centipoises.

Each run comprised two parts, an untreated (control) flood and a treated flood. All displacements were performed in a constant temperature box at  $35 \pm 1^\circ\text{C}$ .

The bed was first saturated with oil, at the same flow rate used in the run to follow, until no more water was displaced. The total quantity of water produced was a measure of the oil saturation in the bed. The untreated water flood was then carried out, followed by resaturation with oil, and the treated flood. Data were obtained on oil production and bed-pressure drop as a function of the total water injected (cumulative pore volumes throughput) for both treated and untreated floods. The treatment was identical for all runs (0.052 pore volumes of aqueous 0.106N hexyl amine) unless otherwise specified. A treatment such as this is not concentrated enough to result in appreciable effects from interfacial tension depression but strong enough to produce a significant increase in oil recovery as a reverse-wetting agent. In addition, this is the one treatment which Stancell (8) considered as economically feasible. Other treatments investigated did not result in increases in oil recovery commensurate with the cost of the amine and the additional water injection required for its production. In a few of the runs, the same quantity of amine was injected in the oil phase rather than in the aqueous phase. In a few cases this was followed by an equivalent amount of aqueous 0.1N hydrochloric acid.

Amine chromatograms were obtained for all treated floods by titrating samples of the effluent aqueous phase with  $1.6 \cdot 10^{-4}\text{N}$  hydrochloric acid with a pH meter to accurately fix the end point.

Both treated and untreated floods were continued until the fraction of oil in the effluent stream was less than 0.0015. If, at this point, oil masses were still observed moving through the bed, the run was continued until all oil was produced.

#### Microscopic System

The glass-grid micromodel was designed and constructed by Dr. C. C. Mattax (5). It consisted of two glass plates fused together by an annealing process. Prior to assembly, one of the square plates was etched with a rectangular grid of interconnecting capillary grooves spaced 0.266 mm. apart. A typical pore had a bell-shaped cross section and measured  $70\mu$  wide (at the widest point),  $25\mu$  deep (at the deepest point), and  $200\mu$  long. The total pore volume of the model was 0.08 ml. (equivalent to a porosity of 35%), and its permeability was about 6 darcies. The capillary network was provided with inlet and outlet wells at diagonal corners of the plates.

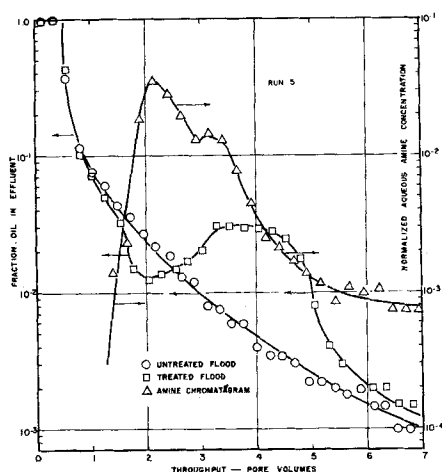


Fig. 3. Effluent oil-fraction curve and amine chromatogram (medium oil-water viscosity ratio).

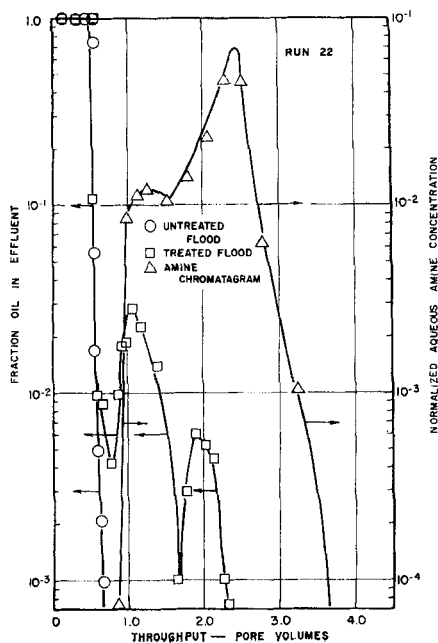


Fig. 5. Effluent oil-fraction curve and amine chromatogram (low oil-water viscosity ratio).

The clean, water-filled micromodel was first saturated with oil (dyed with red soudan III). The oil was displaced with water (with or without 0.1N hexyl amine) at a constant rate with a motor-drive ultramicro buret. Desorption of hexyl amine into water from glass is apparently much more difficult than from sand. In order to hasten desorption, dilute hydrochloric acid was injected in the flood following the hexyl amine. Microscopic observations were made at low power (12-18-100x) to facilitate observations of the formation and propagation of large oil masses. Important phenomena were recorded on 16-mm. color motion-picture film.

## RESULTS AND DISCUSSION

Experimental results from runs on the unconsolidated sand packs are presented in Table 1. The increase in oil recovery (expressed as percentage of pore volume) relative to the untreated flood ( $\Delta R$ ) is used as a measure of the displacement efficiency.

### Treatment Injection and Viscosity Ratio

In the previous studies by Timmins (6, 10) and Stancell (8), the amine was always injected after 0.25 pore volumes (P.V.) throughput, and the oil-water viscosity ratio was always 7.15.

Figure 1 shows the increase in oil recovery ( $\Delta R$ ) as a function of the stage in the displacement at which amine was injected for the various viscosity ratios examined. The lines are drawn through those points representing runs in columns showing the smallest variation in permeability, generally  $4.34 \pm 0.14$  darcies.

**Oil-Water Viscosity Ratio = 7.15.** Figures 2 and 3 (run 5) represent typical data from runs with a viscosity ratio of 7.15. The oil-desaturation curve (Figure 2) and the effluent oil-fraction curve (Figure 3) both show a period of decreased oil production, relative to the untreated flood, before increased oil production is realized. This period of decreased recovery is coincident with amine arrival at the outflow face of the bed as shown in the amine chromatogram of Figure 3. This is expected, since an alteration of wettability from water wet to oil wet would be expected to cause retention of some oil which would normally be produced. For runs resulting in a net increase in oil recovery, the period of

increased recovery coincided with the arrival of an oil mass at the outflow face of the bed. Oil masses could be observed in the column once formed (owing to differences in the index of refraction between the oil and water) and followed as they moved through the bed. Typical oil masses were 7 to 9 in. long with a diameter of 1 in. or so. In addition, the secondary peak in the amine chromatogram (Figure 3) was coincident with oil-mass production. This reflects the fact that an oil mass containing amine (amine distribution coefficient 4:1 in favor of the oil) is not in equilibrium with the aqueous phase, while still in the bed, owing to the small interfacial area for mass transfer. Since these oil masses are thought to be continuous with very little included water, and it is known that oil and water do not flow simultaneously through the same pore, the available interfacial area for mass transfer is only that of the oil mass boundary. However, when the oil masses pass into the small outlet tube along with surrounding water, they are broken up into small oil globules with a resulting increase in interfacial area. This facilitates rapid equilibration. Thus, oil masses may contain higher amounts of amine than would be specified by the equilibrium distribution coefficient until arrival at the outflow tube from the bed, at which point an excess of amine is dumped into the aqueous phase resulting in a secondary peak in the aqueous amine concentration.

**Oil-Water Viscosity Ratio = 0.485.** Figures 4 and 5 (run 22) represent typical data from runs with an oil-water viscosity ratio of 0.485. The untreated flood oil desaturation curve (Figure 4) differs markedly from that for an oil-water viscosity greater than unity. The curve is sharply discontinuous at water breakthrough, with very little oil produced thereafter. This of course reflects the efficiency of displacement processes where the displacing fluid is more viscous than the displaced fluid. However, it will be noted that for all the viscosity ratios examined the ultimate recovery in the untreated flood was the same. The lower the oil-water viscosity ratio, the sooner this recovery was realized.

The treated oil-desaturation curve of Figure 4 again reflects a period of decreased production before the period of increased production. Water breakthrough occurred earlier in the displacement; amine injected at the start of the flood evidently disrupted the sharp displacement front due to fingering induced by wettability alterations. However, injection of amine later in the displacement did not result in significant differences from the untreated flood. Evidently, wettability alterations occurring in regions where the oil saturation has been reduced to

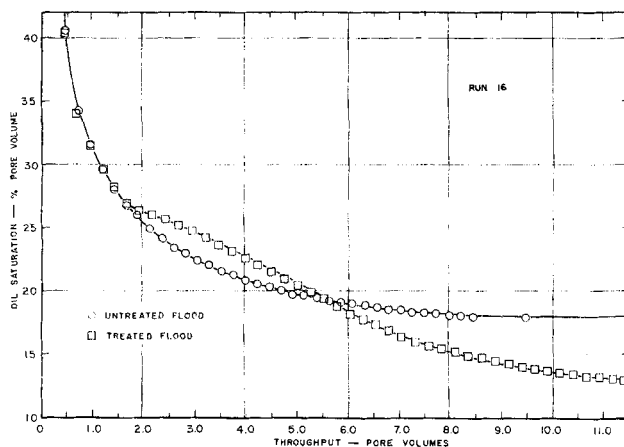


Fig. 6. Oil desaturation curve (high oil-water viscosity ratio).

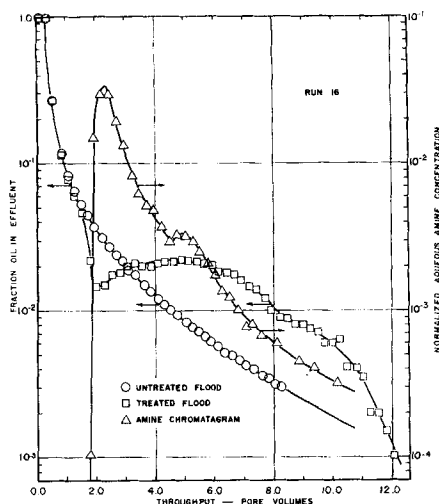


Fig. 7. Effluent oil-fraction cure and amine chromatogram (high oil-water viscosity ratio).

the irreducible minimum value do not effect retention or release of additional oil.

The amine chromatogram (Figure 5) is also distinctly different from chromatograms at higher oil-water viscosity ratios. Here the first peak is coincident with oil mass production rather than the second peak. It is possible that the low-viscosity oil when formed into a mass large enough to be propagated by the hydraulic pressure gradient moves almost as fast as the water phase, thereby passing up the amine band whose partition chromatography is governed primarily by the fixed oil phase (that is, the residual oil never mobilized). It is interesting to note that the amine band arrives at the outflow face after the same number of pore volumes throughput required in runs with higher viscosity oils. In addition, it was noted that the number of pore volumes of injected water necessary to transport the amine through the bed was nearly constant, regardless of the stage of displacement at which amine was injected.

**Oil-Water Viscosity Ratio = 16.60.** Figures 6 and 7 (run 16) represent typical data from runs with an oil-water viscosity ratio of 16.60. These data are very similar to those for a viscosity ratio of 7.15 (Figures 2 and 3), the primary difference being that the ultimate oil recovery is realized much later in the flood for both treated and untreated floods.

**Discussion.** The trends in  $\Delta R$  (increase in oil recovery) with oil viscosity and stage of amine injection (Figure 1) may be explained on the same basis. Apparently, oil-mass formation is only possible if the region undergoing transient adhesion-tension alterations has an oil saturation greater than the irreducible minimum value.

Injection of amine after the irreducible minimum oil saturation had been reached did not result in oil-mass formation. This was confirmed by micromodel studies in which oil was first displaced by water until no more oil was produced, and then amine was injected making the oil the wetting phase (observed as pendular rings in the micromodel). The oil was highly saturated with amine, but the interfacial tension was not low enough for the hydraulic forces to force oil out of the pendular rings. Upon desorption of amine, the oil was displaced from pendular rings but existed as trapped globules. In effect, the alteration in wettability from water wet to oil wet and back again produced no net change in oil configuration and certainly no oil-mass formation.

For high oil-water viscosity ratios, the irreducible oil saturation was reached much later in the flood, thereby

permitting oil-mass formation at a much later stage of oil displacement. The higher the oil-water viscosity ratio, the more diffuse was the displacement front (due to fingering). This may explain why amine treatments in beds containing more viscous oils resulted in larger increases in oil recovery. Under these circumstances, a mobility ratio normally regarded as unfavorable in simple water flooding becomes favorable. The more viscous the oil, the more valuable the treatment appears. The results are comparable to those obtained by Wagner and Leach (12), who found that wettability reversal floods (oil wet to water wet) were more effective for more viscous oils.

Oil masses observed in the sand packs and in the micromodel can be formed either as a result of amine adsorption or as a result of amine desorption. If oil masses were formed as a result of amine adsorption, the most likely mechanism would involve mobilization of excess oil (over and above the irreducible minimum saturation) through interfacial tension depression. The mobilized oil then moves down stream to coalesce with oil still immobilized. However, it is unlikely that this could occur for the higher-viscosity oils, since the amine band would always move faster than the mobilized oil. Stancell (8) reported seeing oil masses in the micromodel during amine adsorption, but he was never able to observe the process of formation. Perhaps the oil masses were a result of preferential flow through certain regions of the micromodel. The authors attempted to view this process but were unsuccessful except with very low-viscosity oil; even then, the coalescence did not result in a stable oil-mass configuration. The fact that injection of amine after the irreducible minimum oil saturation had been reached did not result in oil-mass formation or an increase in oil production indicates that this mechanism is highly improbable. Oil cannot be mobilized to move downstream and contact immobile oil, for if the oil downstream had become immobile, the oil upstream would already have been at the irreducible minimum oil saturation and hence unaffected by the treatment.

Oil-mass formation was observed more frequently during amine desorption (restoration of water wettability). It is significant that Wagner and Leach (12) obtained increases in oil recovery only through a wettability reversal from oil wet to water wet (comparable to amine desorption). This supports the belief that the basic mechanism responsible for increased oil recovery is similar for these two situations.

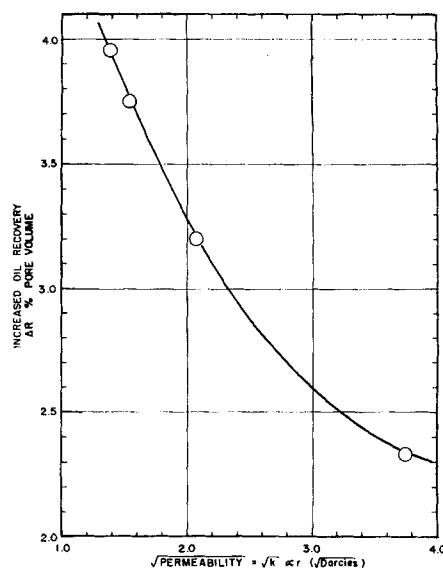


Fig. 8. Effect of hydraulic permeability on increased oil recovery.

The mechanism for oil-mass formation during amine desorption was easily and frequently observed. It was accomplished as a result of wettability gradients established across small pendular ring complexes, which tended to cause inhibition of oil into oil-wet regions from water-wet regions with nearly complete expulsion of water.

Particularly for the more viscous oils, the desorbing water tended to finger through some regions more than others, desorbing amine and causing capillary forces to be directed away from the finger. Two such fingers could squeeze the oil into a continuous mass between the fingers. This resulted in an oil mass across which was imposed a favorable wettability gradient in the direction of flow, the upstream end of the mass being water wet and the downstream end oil wet. A wettability gradient of this sort propagated the mass forward, incorporating additional oil as it moved, until the mass was long enough for hydraulic forces to take over.

As the mass was propagated forward, several interesting phenomena were observed. The area left in the wake of the mass was swept clean of oil. This would not be expected under normal water desorption (no hydrochloric acid) but indicates how treatments followed with hydrochloric acid (runs 13, 29) resulted in additional oil recovery. It was also interesting to note that included water existing within a continuous oil mass remained stationary as the oil mass advanced. This provided a means for expelling water from the oil mass. Other observations indicated that water, included in the oil mass but connected to the boundary of the mass by one or more water channels, tended to be expelled from the mass by oil displacement via capillary action.

As oil masses are propagated through the sand pack or the micromodel, they become longer and thinner owing to the hydraulic forces and capillary forces in interplay. This resulted in some shedding from the tail of the oil mass due to pinching off small segments of oil by capillary action. This may explain the results of run 7. After producing a  $\Delta R$  of 3.05% P.V., injection of amine in an oil slug (a preformed oil mass) did not result in

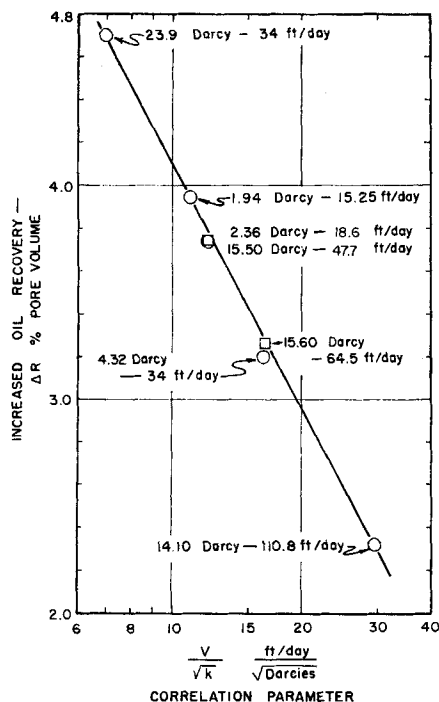


Fig. 9. Correlation of increased oil recovery with flow rate and hydraulic permeability.

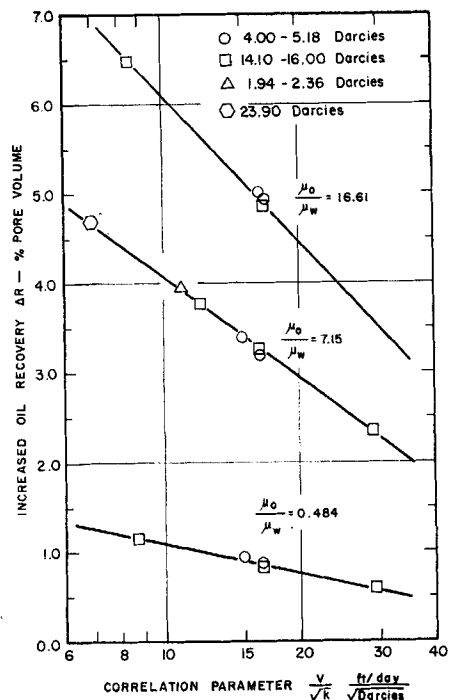


Fig. 10. Correlation of increased oil recovery with flow rate, hydraulic permeability, and oil-water viscosity ratio.

additional oil recovery, and recovery of the injected oil mass was incomplete. Evidently shedding over compensated for the additional oil incorporated in the mass.

It is interesting to note that for low-viscosity oil (run 28), injection of amine in the oil phase at the start of the displacement resulted in less oil recovery than when injected in the aqueous phase (run 22). Evidently, the induced fingering by the amine and slow diffusion of amine from the oil to the water resulted in very little extra oil-mass formation. However, when followed immediately with an equivalent amount of 0.1N hydrochloric acid (run 29), the increase in oil recovery was more than twice as great as with aqueous amine injection. Evidently, the displacement front remains relatively sharp in such a process with a favorable wettability gradient, the front itself being water wet with the oil ahead of the front occupying oil-wet pores. This is very similar to the situation examined by Wagner and Leach (12) and gave similar results.

#### Hydraulic Permeability

In the previous studies by Timmins (6, 10) and Stan-cell (8), all columns were packed with 140- to 200-mesh Ottawa sand. If capillary forces are significant in oil-mass formation and propagation, a decrease in the permeability of the medium (that is, the average pore diameter) should result in larger recoveries.

**Runs at Equivalent Pressure Drop.** Figure 8 shows the increase in oil recovery ( $\Delta R$ ) as a function of the hydraulic permeability (plotted as the  $\sqrt{k}$  which is proportional to the average pore diameter). All runs (5, 32, 33, 35) were carried out at flow rates such that the pressure drops would be equivalent. This was done so that fingering processes would be comparable. An oil-water viscosity ratio of 7.15 was used throughout with amine injection at 0.0 P.V.

The fact that ( $\Delta R$ ) decreases with increasing permeability at constant hydraulic pressure gradient provides further support for the argument that capillary pressure gradients (which also decrease with increasing permeabil-

ity or pore size) are primarily responsible for enhanced oil recovery. Alternatively, however, one might postulate that, as permeability decreases, the interfacial solid-liquid or liquid-liquid specific surface area increases, and with it, the rate of amine interchange between the phases; this enhanced rate of equilibration of oil, solid, and water with amine might lead to increased oil movement. This latter explanation is, in the opinion of the authors, less satisfactory than the former, inasmuch as the micromodel studies have shown quite clearly that macroscopic oil-mass formation during amine desorption precedes oil mobilization, and that it is poor mass transfer of amine from oil to water which sustains oil-mass movements. Once macroscopic oil masses have formed, it is doubtful whether oil-water amine exchange is much influenced by the pore size of the medium.

Run 34 was performed on a column with a permeability of 24 darcies. Since the flow rate required for an equivalent pressure drop was higher than the capacity of the pump, this run was made at the same flow rate as run 5 and resulted in a much higher recovery. This seems to contradict the results of Stancell (8), who found that a low flow rate (4 ft./day) resulted in no increase in oil recovery. In this case, however, oil masses were observed to form but to stagnate in the medium. It is believed that, at such exceedingly low flow rates, it is impossible to produce a significant amine gradient in the flow direction and thereby develop a suitable wettability gradient.

**Discussion.** If the mechanism for oil-mass formation observed in the micromodel is correct, one might expect that the interplay between hydraulic forces and capillary forces is important to oil-mass formation. If the flow rate is too high, collection of oil into an oil mass via capillary forces directed perpendicular to the direction of flow would not be permitted. This may explain why run 11 performed on a bed of nonuniform permeability gave a greater increase in recovery than its equivalent, run 5. The thin layers of relatively loose packing may have aided in the collection of oil into larger masses. If the velocity of oil in the direction of flow is divided by the velocity of oil perpendicular to the direction of flow (resulting in collection) the ratio is proportional to

$$\frac{U_y}{U_x} \propto \left[ 1 + \frac{r\Delta P}{4\gamma_{ow}} \cos \theta \right]$$

For runs conducted at an equivalent pressure drop ( $\Delta P$ ), oil-mass formation should be favored by smaller pores (lower permeability). This is supported by the results of Figure 8. However, if  $\Delta P$  is not held constant, the important factor is the ratio of the flow rate ( $V$ ) to the average pore radius ( $r$ ), since the pressure drop ( $\Delta P$ )

$$\Delta P \propto \frac{V}{r^2}$$

Therefore, a reasonable correlation parameter might be  $V/r$  or  $V/\sqrt{k}$ , where  $k$  is the hydraulic permeability. This, in essence, is a ratio of the hydraulic forces to the capillary forces.

Figure 9 is a plot of the  $\Delta R$  for the runs mentioned previously (5, 32-35) as a function of the correlation parameter. In order to check this correlation, two additional runs were carried out on the 15-darcy sand at lower flow rates (runs 36 and 37).

Since the agreement was good, it was decided to try other viscosity ratios at the same value of the correlation parameter ( $V/\sqrt{k}$ ) but for sands of differing permeabilities. Run 38 was designed to compare with run 22 and run 41 with run 16. Again, the agreement was good, so

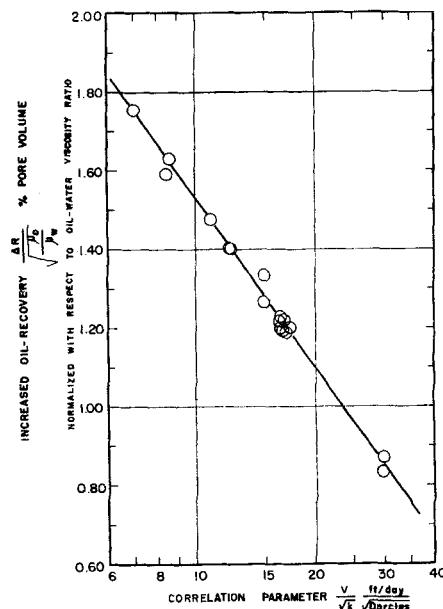


Fig. 11. Correlation of increased oil recovery (normalized with respect to oil-water viscosity ratio) with flow rate and hydraulic permeability.

three other runs (39, 40, 42) were performed to determine the trends in  $\Delta R$  with  $V/\sqrt{k}$  for the three viscosity ratios. The results are presented in Figure 10.

It will be noted that the increase in oil recovery ( $\Delta R$ ) for a given value of the correlation parameter ( $V/\sqrt{k}$ ) varies approximately as the square root of the oil-water viscosity ratio. Thus, the values of  $\Delta R$  may be normalized with respect to the oil-water viscosity ratio by plotting  $(\Delta R)/(\sqrt{u_o/u_w})$  as a function of  $V/\sqrt{k}$ . All of the data presented in Table 1 for amine injection in the aqueous phase at 0.0 P.V. are plotted in Figure 11.

The correlation is unexpectedly good and the linearization with semilogarithmic coordinates convenient. While the use of  $V/\sqrt{k}$  as a correlation parameter appears to be justified from a simple physical model of oil-mass formation as observed in the micromodel, it should be noted that the ultimate correlation is largely empirical. Further study and analysis will be needed to establish whether the correlation is a general one and if it has any theoretical basis.

## CONCLUSIONS

1. The increases in oil recovery from unconsolidated sands effected by hexylamine injection during water displacement are the result of formation and propagation of large continuous oil masses under favorable wettability gradients.

2. Oil-mass formation, and increased oil recovery, are not observed if the oil saturation in the medium undergoing transient adhesion-tension alterations is at its irreducible minimum value. Hence, early injection of amine favors increased oil recovery.

3. Oil-mass formation, and increased oil recovery, are favored with more viscous oils, and the increase in oil recovery seems to be proportional to the square root of the oil-water viscosity ratio.

4. Oil-mass formation appears to take place primarily during amine desorption, as the medium is returned from oil-wet to water-wet conditions.

5. The importance of capillary forces in oil-mass formation and propagation is reflected in the increase in oil recovery with decreasing hydraulic permeability.

6. In the range of the variables investigated, an increase in flow rate is detrimental to oil-mass formation and propagation. The data may be correlated by plotting the increase in oil recovery as a function of the ratio of the flow rate to the square root of the permeability (essentially the ratio of the hydraulic forces to the capillary forces).

#### ACKNOWLEDGMENT

Financial assistance from the American Petroleum Institute (A.P.I. Grant in Aid No. 97) is gratefully acknowledged. The advice, guidance, and suggestions of Dr. F. M. Perkins, Jr., and later Dr. C. W. Arnold of Humble Oil and Refining Company, A.P.I. Liaison Representatives for this project, and of Dr. R. O. Leach of Pan American Petroleum Corp. are deeply appreciated. The glass-grid micromodel was courteously provided by Dr. C. C. Mattax who was responsible for its design and construction.

#### NOTATION

- $k$  = hydraulic permeability, darcies  
 $\Delta P$  = pressure drop across column, lb./sq. in.  
 $P.V.$  = pore volume, ml.  
 $\Delta R$  = increase in oil recovery relative to an untreated water-oil displacement, % pore volume  
 $r$  = average pore radius,  $\mu$   
 $U_s$  = velocity of oil perpendicular to direction of flow, ft./day  
 $U_v$  = velocity of oil in direction of flow, ft./day  
 $V$  = flow rate, ft./day  
 $\gamma_{ow}$  = oil-water interfacial tension, dynes/cm.

- $\mu_o$  = viscosity of oil phase at 35°C., centipoises  
 $\mu_w$  = viscosity of water phase at 35°C., centipoises  
 $\theta$  = contact angle (viewed through aqueous phase), deg.

#### LITERATURE CITED

- Caro, R. A., J. C. Calhoun, and R. F. Nielsen, *Oil Gas J.*, **51**, 62 (1952).
- Johansen, R. T., N. H. Dunning, and J. W. Beaty, *Penn. State Univ. Mineral Ind. Exp. Sta. Bull.* **68** (1955).
- Kyte, J. R., and L. A. Rapoport, Am. Inst. Mining Engrs., Preprint No. 929G, Dallas, Texas (October, 1957).
- Leach, R. O., O. R. Wagner, H. W. Wood, and C. F. Harpke, *J. Petrol. Technol.*, **14**, 206 (1962).
- Mattax, C. C., and J. R. Kyte, *Oil Gas J.*, **59**, 42 (1961).
- Michaels, A. S., and R. S. Timmins, *Trans. Am. Inst. Mining Engrs.*, **219**, 150 (1960).
- Stahl, C. D., J. C. Calhoun, F. W. Preson, and R. F. Nielsen, *Penn. State Univ. Minerals Ind. Exp. Sta. Bull.* **59** (1951).
- Stancell, A., Sc.D. thesis, Mass. Inst. Technol., Cambridge, Massachusetts (1962).
- Taber, J. J., *Trans. Am. Inst. Mining Engrs.*, **213**, 186 (1958).
- Timmins, R. S., Sc.D. thesis, Mass. Inst. Technol., Cambridge, Massachusetts (1959).
- Torrey, P. D., "Evaluation of Secondary Recovery Prospects," Economics of Petroleum Exploration, Development, and Property Evaluation, Prentis Hall, Englewood Cliffs, New Jersey (1961).
- Wagner, O. R., and R. O. Leach, *Trans. Am. Inst. Mining Engrs.*, **216**, 65 (1959).

Manuscript received June 30, 1964; revision received December 29, 1964; paper accepted January 13, 1965. Paper presented at A.I.Ch.E. Pittsburgh meeting.

# Local Parameters in Cocurrent Mercury-Nitrogen Flow: Parts I and II

L. G. NEAL and S. G. BANKOFF

Northwestern University, Evanston, Illinois

An experimental study was made in a cocurrent vertical mercury-nitrogen flow of local parameters, including local liquid velocity and gas fraction. In Part I the pertinent quantities are carefully defined and power-law continuity expressions derived. A description is given of the apparatus, including a simple local liquid velocity probe. In Part II experimental velocity and void profiles are given for the mercury-nitrogen flow. The regime is slug flow, but the slugs are not axisymmetrical, on account of the nonwetted walls. Intensities of density and liquid velocity fluctuations are computed for the first time and a comparison made with Levy's mixing-length theory.

#### PART I

Because of their attractiveness in the design of compact power plants, considerable attention has been focussed recently on the mechanics of cocurrent flows in pipes or channels of a liquid metal and a gaseous phase. In some ways, these flows exhibit unique features not found to such a pronounced degree in two-phase flows involving

the usual aqueous or organic media. For example, because of the high surface energy and density of liquid metals, the slug flow regime normally prevails. Except in special circumstances, moreover, the gas concentrates at the walls of the pipe, owing to the poor wetting properties of liquid metals in contact with most engineering surfaces. This gives rise to asymmetric (frequently helicoidal) gas slugs which hug the pipe wall, in contrast to the axisymmetric slugs observed in aqueous flows.

L. G. Neal is with the TRW Space Technology Laboratories, Redondo Beach, California.